First order surface grating fiber coupler under the period chirp and apodization functions variations effects

Alsharef Mohammad[1], Mohammed S. Alzaidi[1], Mahmoud M. A. Eid[1], Vishal Sorathiya[2], Sunil Lavadiya[2], Shobhit K. Patel[3,4], Ahmed Nabih Zaki Rashed[5]
[1]Department of Electrical Engineering, College of Engineering, Taif University, Taif, Kingdom of Saudi Arabia
[2]Department of Information and Communication Technology, Marwadi University, Rajkot, India
[3]Department of Electronics and Communication Engineering, Marwadi University, Rajkot, India
[4]Department of Computer Engineering, Marwadi University, Rajkot, India
[5]Department Electronics and Electrical Communications Engineering, Faculty of Electronic Engineering, Menoufia University, Menofia, Egypt

Article Info

Article history:

Received Aug 25, 2021
Revised Dec 1, 2021
Accepted Dec 17, 2021

Keywords:

Apodization function
Fiber coupler
Period chirp
Surface grating

ABSTRACT

The paper has demonstrated the first order surface grating fiber coupler under the period chirp and apodization functions variations effects. The Fiber coupler transmittivity/reflectivity, the fiber coupler grating index change and the fiber coupler mesh transmission cross-section are clarified against the grating length with the quadratic/cubic root period chirp and Gaussian/uniform apodization functions. The fiber coupler delay and dispersion are simulated and demonstrated with grating wavelength with quadratic/cubic root period chirp and Gaussian/uniform apodization function. As well as the fiber coupler output pulse intensity is simulated against the time period with the quadratic/cubic root period chirp and Gaussian/uniform apodization function. The fiber coupler peak intensity variations against the transmission range variations is also demonstrated by OptiGrating simulation software.

Corresponding Author:

Ahmed Nabih Zaki Rashed
Department Electronics and Electrical Communications Engineering, Faculty of Electronic Engineering
Menoufia University
Menofia, Egypt
Email: alihas@upm.edu.my

1. INTRODUCTION

The single mode fiber (SMF) is also known as fundamental or monomode fiber. The condition for verifying the single mode operation is obtained by the V-number of fibers as V≤2.405. In SMFs, the normalized frequency is < 2.405. The major method for minimizing the modal dispersion is to reduce the core diameter until the fiber propagates efficiently single mode only [1]-[5]. The SMF has a smaller core diameter (about 10 μm) with a 125 μm cladding diameter. The typical core diameters are from 5 to 10 μm and the difference of refractive index is very small [6]-[8]. Because its core is very narrow compared to the light wavelength being used, the SMF permits only single light path or mode to transmit through it [9], [10].

Thus, the SMF does not suffer from mode delay differences. Its extreme smaller core diameter makes the interconnection or splicing of cables and interfacing or termination with optical source and detector or the coupling and launching of light into the SMF more difficult requiring more accuracy. Therefore, the fabrication of SMF is very difficult and costly [11]-[17]. The SMFs are used only with laser diode (LDs) due to the high coupling losses accompanying with light emitting diodes (LEDs). The SMF has a larger capacity to transmit data in a certain fidelity over longer distances because it exhibits transmission attenuation lower than the multi mode fibers (MMF) and does not suffer from modal dispersion caused by the multiple modes as occurred in the MMF [18]-[23]. So, they are used for high bandwidth long haul communications like high-speed local area network (LAN) and wide area network (WAN) backbones where the amplifier/repeater span must be maximized. However, the SMFs are affected by chromatic dispersion which can limit the system performance at higher data rates [24]-[30].

2. MODEL RESEARCH DESCRIPTION

Fiber coupler has two fibers construction as clarified in Figure 1. The first fiber basic construction that has three regions as illustrated in Figure 1(a). The first region is the core which its linear index ranges from 1.455 to 1.46 with the width of 2 µm. The second region is the cladding which its parabolic index ranges from 1.452 to 1.456 with the width of 8 µm. The third region is the overcladding which its Gaussian index has max index of 1.46, normalized full width at half maximum (FWHM) of 10 with the width of 12 µm.

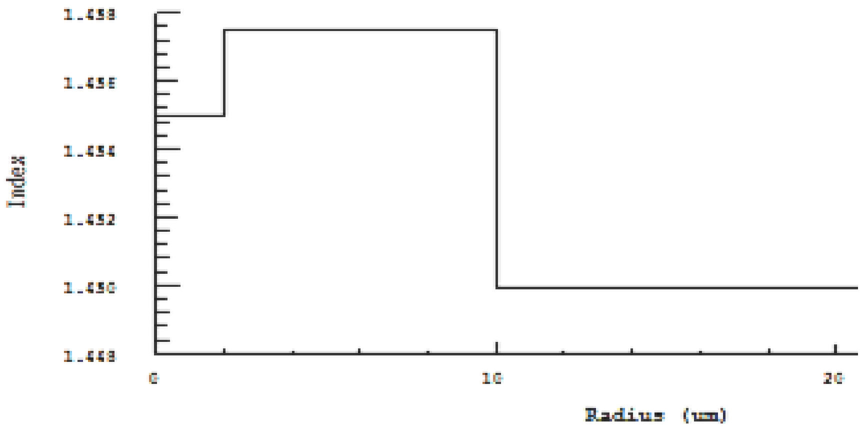

(a)

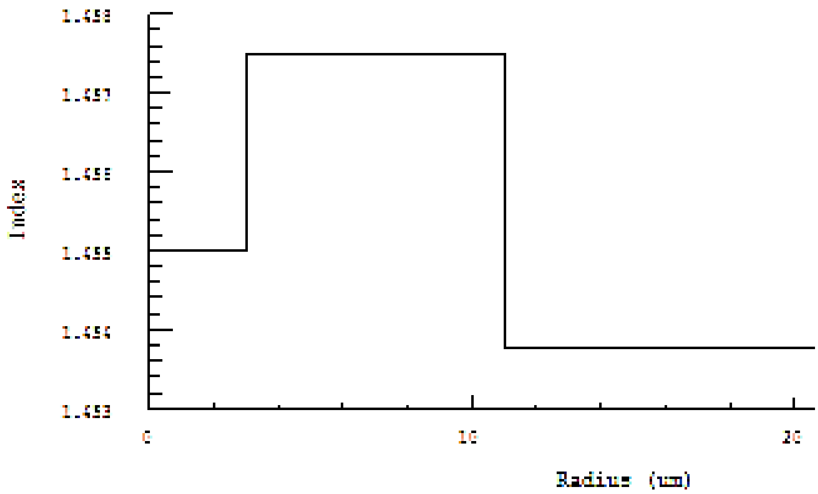

(b)

Figure 1. Fiber: (a) 1 basic construction and (b) 2 basic construction

The basic second fiber construction that has three regions as demonstrated in Figure 1(b). The first region is the core which its linear index ranges from 1.456 to 1.459 with the width of 3 µm. The second region is the cladding which its parabolic index ranges from 1.454 to 1.458 with the width of 8 µm. The third region is the overcladding which its exponential index ranges from 1.450 to 1.452 with the width of 15 µm. The average index modulation in the linear relation is estimated by [1], [3], [5], [9], [19]:

$$\Delta n_0 = \frac{z - 0.5L}{L}\Delta \quad (1)$$

with Δ is the total chirp, L is the grating length. Where the grating period chirp in the linear, quadratic, square root and cubic root relations are given by [2], [4], [7], [9], [11], [12]:

$$\Lambda(z) = \Lambda_0 - \frac{z-0.5L}{L}\Delta \text{ [linear]} \quad (2)$$

$$\Lambda(z) = \Lambda_0 - \left[\left(\frac{z}{L}\right)^2 - \frac{1}{4}\right]\Delta \text{ [Quadratic]} \quad (3)$$

$$\Lambda(z) = \Lambda_0 - \left[\sqrt{\frac{z}{L}} -- \frac{1}{\sqrt{2}}\right]\Delta \text{ [Square root]} \quad (4)$$

$$\Lambda(z) = \Lambda_0 - \left[\sqrt[3]{\frac{z}{L}} - \frac{1}{\sqrt[3]{2}}\right]\Delta \text{ [Cubic root]} \quad (5)$$

where the uniform and Gaussian grating apodization functions are calculated by [1], [4], [7], [10], [12]:

$$\Lambda(z) = 1 \text{ [Uniform]} \quad (6)$$

$$\Lambda(z) = exp\left[-ln\,2\,.\left(\frac{2(z-0.5L)}{SL}\right)\right] \text{ [Gaussian]} \quad (7)$$

with S is the taper parameter and z is the radial distance.

3. RESULTS WITH DISCUSSION

We have been simulated the fiber coupler transmittivity/reflectivity, the fiber coupler grating index change and the fiber coupler mesh transmission cross-section against the grating length with the quadratic/cubic root period chirp and uniform/Gaussian apodization functions. Besides the fiber coupler delay and dispersion are demonstrated against the grating wavelength with the cubic root/quadratic period chirp and uniform/Gaussian apodization functions. The fiber coupler output pulse intensity is simulated clearly against the time period with the cubic root/quadratic period chirp and uniform/Gaussian apodization functions.

Figure 2 clarifies the fiber coupler transmittivity/reflectivity against the grating length with the quadratic period chirp and Gaussian apodization function. The fiber coupler transmittivity, reflectivity are approximation 0.998, 0.002 respectively at 8000 μm grating length. The fiber coupler transmittivity/ reflectivity with grating length with the cubic root period chirp and uniform apodization function which is clarified in Figure 3. The fiber coupler transmittivity, reflectivity is approximation 0.996, 0.004 respectively at 8000 μm grating length. The fiber coupler transmittivity/reflectivity is enhanced with the quadratic period chirp and Gaussian apodization function than the cubic root period chirp and uniform apodization function.

Figure 4 indicates the fiber coupler grating index change against the grating length with the quadratic period chirp and Gaussian apodization function. The peak grating index change is achieved at 5000 μm grating length which it is 0.0010. With the grating period changes from 0.531998 μm to 0.533219 μm.

Where the fiber coupler grating index change against the grating length with the cubic root period chirp and uniform apodization function is clarified in Figure 5. The peak grating index change is almost constant at a value of 0.00025. With the grating period changes from 0.614401 μm to 0.614473 μm.

Figure 6 shows the fiber coupler mesh transmission cross-section with grating length with the quadratic period chirp and Gaussian apodization function. The fiber coupler mesh transmission cross section values varies from 11.8 μm to 55.6 μm. Figure 7 illustrates the fiber coupler mesh transmission cross-section with grating length with the cubic root period chirp and uniform apodization function. But the fiber coupler mesh transmission cross section values varies from 11.65 μm to 55.32 μm.

Figure 8 demonstrates the fiber coupler delay versus the grating wavelength with the quadratic period chirp and Gaussian apodization function. The max fiber coupler transmission delay is 3 ps at 1.51 μm grating wavelength and the min fiber coupler transmission delay is -1.8 ps at 1.6 μm grating wavelength. The fiber coupler reflection varies in oscillation values along the grating wavelength. Figure 9 illustrates the fiber coupler delay against the grating wavelength with the cubic root period chirp and uniform apodization function. The max fiber coupler transmission delay is 2.85 ps at 1.51 μm grating wavelength and the min fiber coupler transmission delay is approximation -1.9342 ps at 1.6 μm grating wavelength. The fiber coupler reflection is zero along the grating wavelength. The fiber coupler delay is enhanced with the cubic root period chirp and uniform apodization function than the quadratic period chirp and Gaussian apodization function.

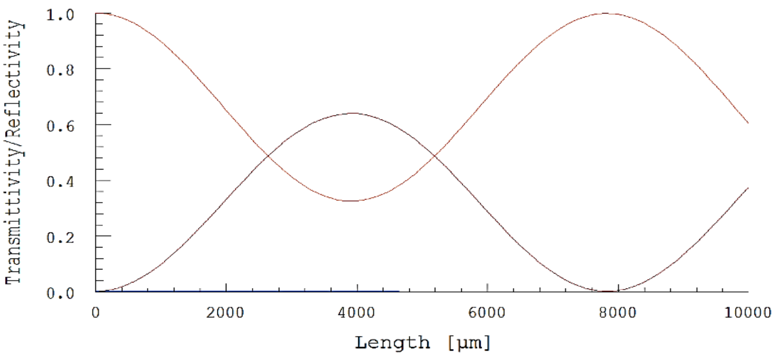

Figure 2. Fiber coupler transmittivity/Reflectivity against the grating length with the quadratic period chirp and Gaussian apodization function

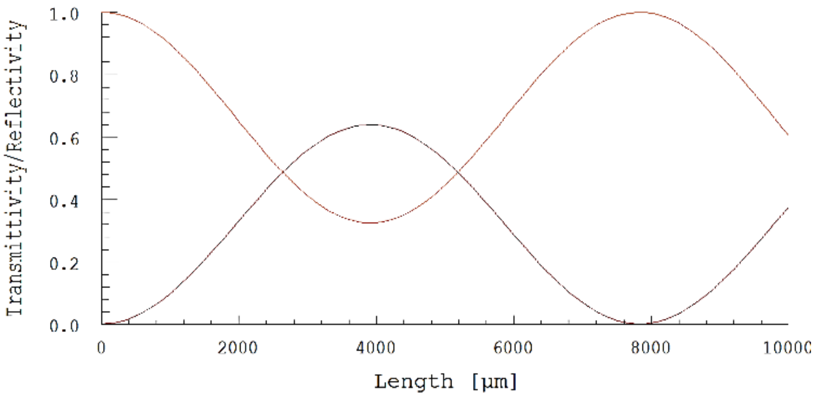

Figure 3. Fiber coupler transmittivity/Reflectivity against the grating length with the cubic root period chirp and uniform apodization function

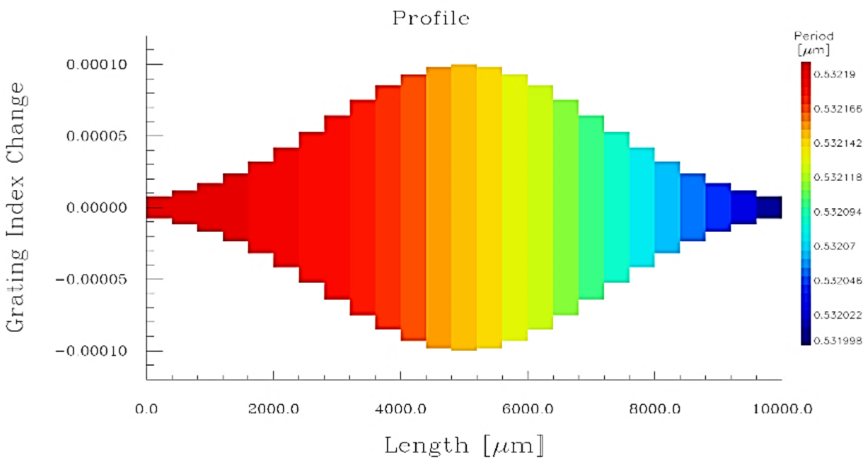

Figure 4. Fiber coupler grating index change against the grating length with the quadratic period chirp and Gaussian apodization function

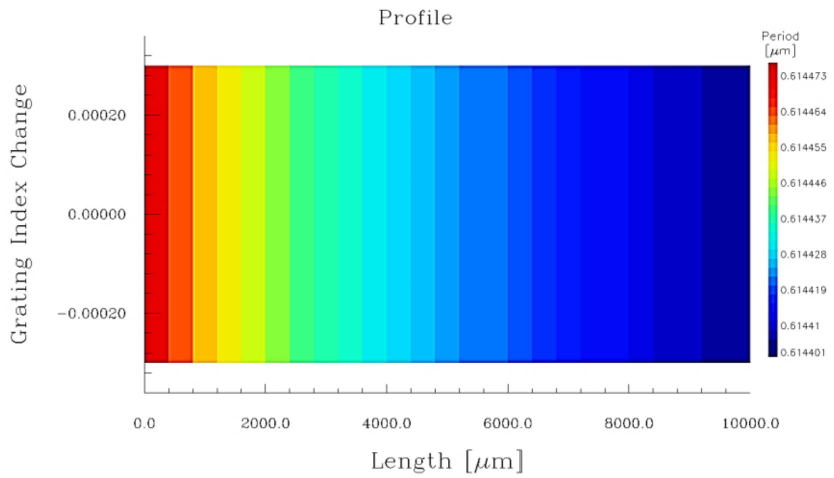

Figure 5. Fiber coupler grating index change against the grating length with the cubic root period chirp and uniform apodization function

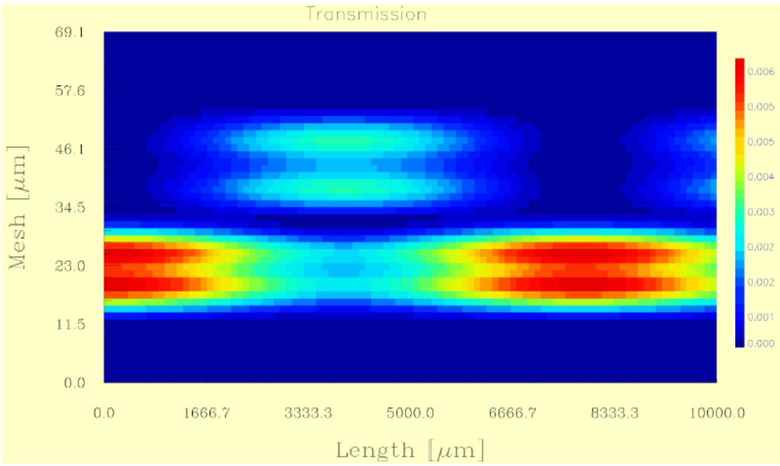

Figure 6. Fiber coupler mesh transmission cross-section with grating length with the quadratic period chirp and Gaussian apodization function

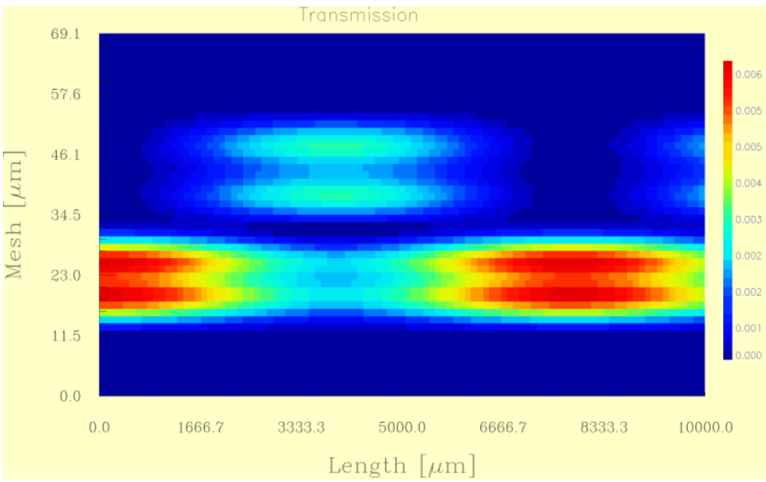

Figure 7. Fiber coupler mesh transmission cross-section with grating length with the cubic root period chirp and uniform apodization function

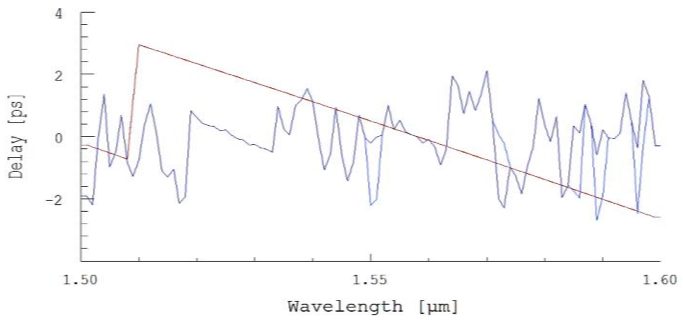

Figure 8. Fiber coupler delay versus the grating wavelength with the quadratic period chirp and Gaussian apodization function

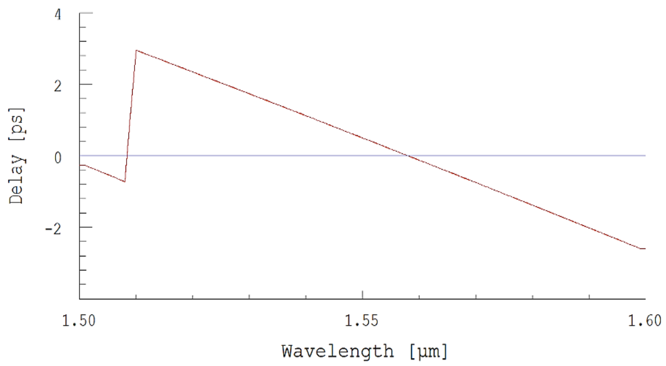

Figure 9. Fiber coupler delay versus the grating wavelength with the cubic root period chirp and uniform apodization function

Figure 10 illustrates the fiber coupler dispersion versus the grating wavelength with the quadratic period chirp and Gaussian apodization function. The max fiber coupler transmission dispersion is 1.865 ps/km at 1.51 μm grating wavelength and the min fiber coupler transmission dispersion is approximation -0.1243 ps/km from the grating wavelength of 1.51 μm to 1.6 μm. The fiber coupler reflection varies in oscillation values along the grating wavelength.

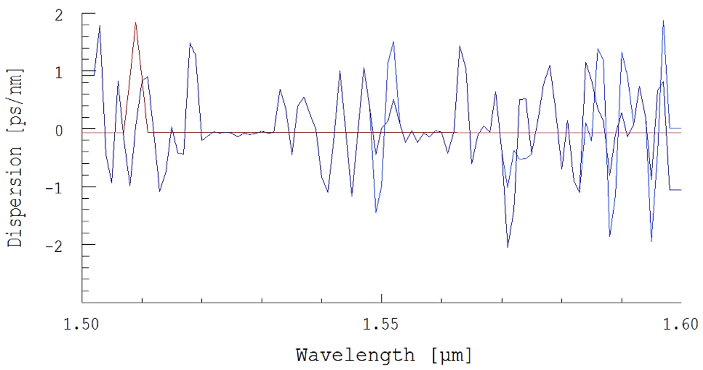

Figure 10. Fiber coupler dispersion against the grating wavelength with the quadratic period chirp and Gaussian apodization function

Figure 11 illustrates the fiber coupler delay against the grating wavelength with the cubic root period chirp and uniform apodization function. The max fiber coupler transmission delay is 1.9832 ps/km at 1.51 μm grating wavelength and the min fiber coupler transmission dispersion is approximation -0.1654 ps/km from the grating wavelength of 1.51 μm to 1.6 μm. The fiber coupler reflection is zero along the grating wavelength. The fiber coupler dispersion is enhanced with the cubic root period chirp and uniform apodization function than the quadratic period chirp and Gaussian apodization function.

Figure 12 demonstrates the fiber coupler output pulse intensity versus the time period with the quadratic period chirp and Gaussian apodization function. The fiber coupler output pulse intensity peak is 0.6 with narrow shrinking. Figure 13 clarifies the fiber coupler output pulse intensity against the time period with the cubic root period chirp and uniform apodization function. The fiber coupler output pulse intensity peak is 0.5923 with wide shrinking. The fiber coupler output pulse intensity can be upgraded with the quadratic period chirp and Gaussian apodization function than the cubic root period chirp and uniform apodization function. Figure 14 clarifies the max fiber coupler pulse position against the transmission range. The max pulse value at zero position is 0.993092 with the ripple factor of unity. The fiber coupler bandwidth by using Figure 14 can be estimated to be 45000 nm.

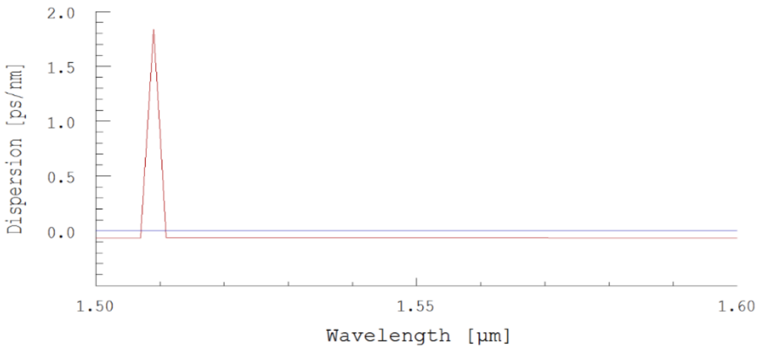

Figure 11. Fiber coupler dispersion against the grating wavelength with the cubic root period chirp and uniform apodization function

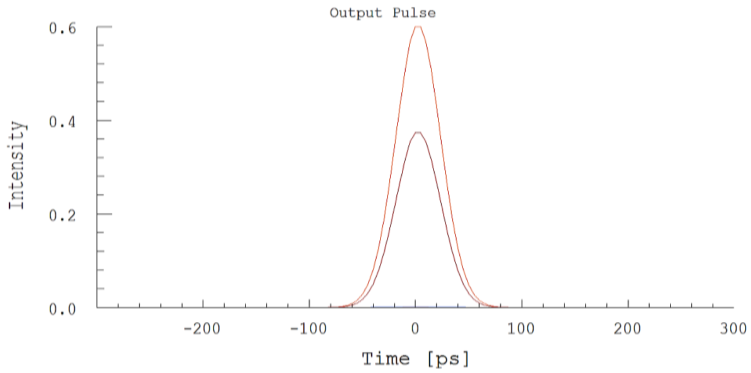

Figure 12. Fiber coupler output pulse intensity against the time period with the quadratic period chirp and Gaussian apodization function

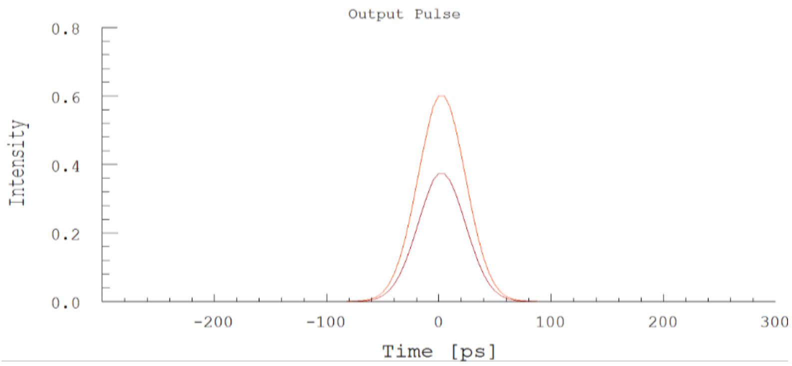

Figure 13. Fiber coupler output pulse intensity against the time period with the cubic root period chirp and uniform apodization function

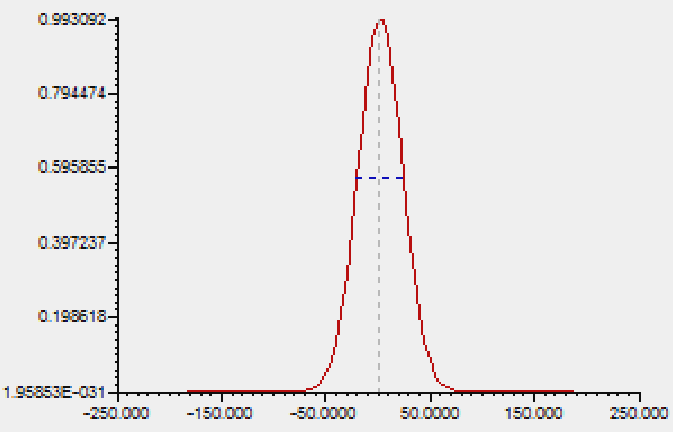

Figure 14. Fiber coupler peak intensity variations against the transmission range variations

4. CONCLUSION

We have simulated the first order surface grating fiber coupler under the period chirp and apodization functions variations effects by OptiGrating. The fiber coupler bandwidth is 45 µm through this study. The fiber coupler output pulse intensity can be upgraded with the quadratic period chirp and Gaussian apodization function than the cubic root period chirp and uniform apodization function. The fiber coupler delay, dispersion are enhanced with the cubic root period chirp and uniform apodization function than the quadratic period chirp and Gaussian apodization function. As well as the fiber coupler transmittivity/Reflectivity is enhanced with the quadratic period chirp and Gaussian apodization function than the cubic root period chirp and uniform apodization function.

REFERENCES

[1] S. E. Miller and I. P. Kaminow, *Optical fiber telecommunications II*. Boston: Academic Press, 1988.
[2] W.-P. Huang, "Coupled-mode theory for optical waveguides: an overview," *Journal of the Optical Society of America A*, vol. 11, no. 3, p. 963, Mar. 1994, doi: 10.1364/JOSAA.11.000963.
[3] D. Marcuse, *Principle of optical fiber measurements*, 1st Editio. Elsevier, 1981.
[4] M. J. Adams, *An introduction to Optical Waveguides*. John Wiley & Sons, 1981.
[5] A. Yariv, "Coupled-mode theory for guided-wave optics," *IEEE Journal of Quantum Electronics*, vol. 9, no. 9, pp. 919–933, Sep. 1973, doi: 10.1109/JQE.1973.1077767.
[6] M. M. A. Eid and A. N. Z. Rashed, "Numerical simulation of long-period grating sensors (LPGS) transmission spectrum behavior under strain and temperature effects," *Sensor Review*, vol. 41, no. 2, pp. 192–199, May 2021, doi: 10.1108/SR-10-2020-0248.
[7] K. O. Hill and G. Meltz, "Fiber Bragg grating technology fundamentals and overview," *Journal of Lightwave Technology*, vol. 15, no. 8, pp. 1263–1276, 1997, doi: 10.1109/50.618320.
[8] T. Erdogan, "Fiber grating spectra," *Journal of Lightwave Technology*, vol. 15, no. 8, pp. 1277–1294, 1997, doi: 10.1109/50.618322.
[9] F. Ouellette, "Dispersion cancellation using linearly chirped Bragg grating filters in optical waveguides," *Optics Letters*, vol. 12, no. 10, p. 847, Oct. 1987, doi: 10.1364/OL.12.000847.
[10] G. P. Agrawal and S. Radic, "Phase-shifted fiber Bragg gratings and their application for wavelength demultiplexing," *IEEE Photonics Technology Letters*, vol. 6, no. 8, pp. 995–997, Aug. 1994, doi: 10.1109/68.313074.
[11] A. Galvanauskas, M. E. Fermann, D. Harter, K. Sugden, and I. Bennion, "All-fiber femtosecond pulse amplification circuit using chirped Bragg gratings," *Applied Physics Letters*, vol. 66, no. 9, pp. 1053–1055, Feb. 1995, doi: 10.1063/1.113571.
[12] L. R. Chen, S. D. Benjamin, P. W. E. Smith, and J. E. Sipe, "Ultrashort pulse reflection from fiber gratings: a numerical investigation," *Journal of Lightwave Technology*, vol. 15, no. 8, pp. 1503–1512, 1997, doi: 10.1109/50.618383.
[13] D. A. J. Al-Khaffaf and H. S. R. Hujijo, "High data rate optical wireless communication system using millimeter wave and optical phase modulation," *ARPN Journal of Engineering and Applied Sciences*, vol. 13, no. 23, pp. 9086–9092, 2018.
[14] D. A. J. Al-Khaffaf and I. A. Alshimaysawe, "Miniaturised tri-band microstrip patch antenna design for radio and millimetre waves of 5G devices," *Indonesian Journal of Electrical Engineering and Computer Science*, vol. 21, no. 3, p. 1594, Mar. 2021, doi: 10.11591/ijeecs.v21.i3.pp1594-1601.
[15] A. N. Z. Rashed and A. E.-F. A. Saad, "Different Electro-Optical Modulators for High Transmission-Data Rates and Signal-Quality Enhancement," *Journal of Russian Laser Research*, vol. 34, no. 4, pp. 336–345, Jul. 2013, doi: 10.1007/s10946-013-9359-2.
[16] K. O. Hill, Y. Fujii, D. C. Johnson, and B. S. Kawasaki, "Photosensitivity in optical fiber waveguides: Application to reflection filter fabrication," *Applied Physics Letters*, vol. 32, no. 10, pp. 647–649, May 1978, doi: 10.1063/1.89881.
[17] B. S. Kawasaki, K. O. Hill, D. C. Johnson, and Y. Fujii, "Narrow-band Bragg reflectors in optical fibers," *Optics Letters*, vol. 3, no. 2, p. 66, Aug. 1978, doi: 10.1364/OL.3.000066.
[18] D. K. W. Lam and B. K. Garside, "Characterization of single-mode optical fiber filters," *Applied Optics*, vol. 20, no. 3, p. 440, Feb. 1981, doi: 10.1364/AO.20.000440.
[19] S. Urooj, N. M. Alwadai, A. Ibrahim, and A. N. Z. Rashed, "Simulative study of raised cosine impulse function with Hamming grating profile based Chirp Bragg grating fiber," *Journal of Optical Communications*, Aug. 2021, doi: 10.1515/joc-2021-0062.

[20] I. Bennion, J. A. R. Williams, L. Zhang, K. Sugden, and N. J. Doran, "Uv-written in-fibre Bragg gratings," *Optical and Quantum Electronics*, vol. 28, no. 2, pp. 1263–1276, Feb. 1996, doi: 10.1007/BF00278281.
[21] Y. Zhan, S. Xue, Q. Yang, S. Xiang, H. He, and R. Zhu, "A novel fiber Bragg grating high-temperature sensor," *Optik*, vol. 119, no. 11, pp. 535–539, Aug. 2008, doi: 10.1016/j.ijleo.2007.02.010.
[22] J. Kou, S. Qiu, F. Xu, and Y. Lu, "Demonstration of a compact temperature sensor based on first-order Bragg grating in a tapered fiber probe," *Optics Express*, vol. 19, no. 19, p. 18452, Sep. 2011, doi: 10.1364/OE.19.018452.
[23] N. Liu, Y. Li, Y. Wang, H. Wang, W. Liang, and P. Lu, "Bending insensitive sensors for strain and temperature measurements with Bragg gratings in Bragg fibers," *Optics Express*, vol. 19, no. 15, p. 13880, Jul. 2011, doi: 10.1364/OE.19.013880.
[24] F. Urban, J. Kadlec, R. Vlach, and R. Kuchta, "Design of a Pressure Sensor Based on Optical Fiber Bragg Grating Lateral Deformation," *Sensors*, vol. 10, no. 12, pp. 11212–11225, Dec. 2010, doi: 10.3390/s101211212.
[25] Q. Jiang and D. Hu, "Microdisplacement Sensor Based on Tilted Fiber Bragg Grating Transversal Load Effect," *IEEE Sensors Journal*, vol. 11, no. 9, pp. 1776–1779, Sep. 2011, doi: 10.1109/JSEN.2010.2103399.
[26] B. Gu, M. Yin, A. P. Zhang, J. Qian, and S. He, "Optical fiber relative humidity sensor based on FBG incorporated thin-core fiber modal interferometer," *Optics Express*, vol. 19, no. 5, p. 4140, Feb. 2011, doi: 10.1364/OE.19.004140.
[27] C. Ambrosino *et al.*, "Fiber Bragg Grating and Magnetic Shape Memory Alloy: Novel High-Sensitivity Magnetic Sensor," *IEEE Sensors Journal*, vol. 7, no. 2, pp. 228–229, Feb. 2007, doi: 10.1109/JSEN.2006.886905.
[28] K. Reck, E. V. Thomsen, and O. Hansen, "MEMS Bragg grating force sensor," *Optics Express*, vol. 19, no. 20, p. 19190, Sep. 2011, doi: 10.1364/OE.19.019190.
[29] G. T. Kanellos, G. Papaioannou, D. Tsiokos, C. Mitrogiannis, G. Nianios, and N. Pleros, "Two dimensional polymer-embedded quasi-distributed FBG pressure sensor for biomedical applications," *Optics Express*, vol. 18, no. 1, p. 179, Jan. 2010, doi: 10.1364/OE.18.000179.
[30] M. Moccia, M. Pisco, A. Cutolo, V. Galdi, P. Bevilacqua, and A. Cusano, "Opto-acoustic behavior of coated fiber Bragg gratings," *Optics Express*, vol. 19, no. 20, p. 18842, Sep. 2011, doi: 10.1364/OE.19.018842.

BIOGRAPHIES OF AUTHORS

Dr. Alsharef Mohammad He has been assigned as the head of Electrical Engineering Department at Taif University. His area of interest includes Wireless Communications, Digital Communications, Spread Spectrum Techniques and Continuous Phase Modulation Techniques. He can be contacted at email: M.alsharef@tu.edu.sa.

Dr. Mohammed S. Alzaidi He is currently an Assistant Professor with the Department of Electrical Engineering, Faculty of Engineering, Taif University, Saudi Arabia. He is also the Vice Dean of the Deanship of Scientific Research at Taif University. His research interests include nano molecular communications, wireless communications, signal processing, digital techniques, machine learning, and deep learning. He can be contacted at email: m.alzaidi@tu.edu.sa.

Dr. Mohamoud M. A. Eid Taif University, Electrical Engineering Department, Faculty of Engineering, He joins now the Taif University as an assistant professor in the Electrical Engineering Department, Faculty of Engineering. His interesting research focuses on optical sources, amplifiers, detectors, and sensors, optoelectronic devices. He can be contacted at email: m.elfateh@tu.edu.sa.

Dr. Vishal Sorathiya Marwadi University, Rajkot India. Field of the Graphene-based nano antenna for the IoT and smart sensor applications. His key interest in the field of the reconfigurable antenna for IoT application, solar cell, and photonics devices. He can be contacted at email: vishal.sorathiya9@gmail.com.

Dr. Sunil Lavadiya Marwadi University. He currently works as an assistant professor in department of information and communication engineering, Marwadi University. He can be contacted at email: splavadiya@gmail.com.

Dr. Shobhit K. Patel Ph.D. on Electronics and communication engineering at Charotar University of Science and Technology, Changa, India. He is currently working in the area of photonics, metamaterial, antenna, optics and artificial intelligence. He has been named in the list of "top 2% scientist worldwide identified by Stanford university" in 2021. He can be contacted at email: shobhitkumar.patel@marwadieducation.edu.in.

Prof. Ahmed Nabih Zaki Rashed Faculty of Electronic Engineering, Menoufia University, Egypt. He has Published more than 325 Papers in high impacted Journals and Editor in Many international Journals. Prof. Rashed was selected among the top 2% of scientists published by Stanford University. He can be contacted at email: ahmed_733@yahoo.com.